International Journal of Medical, Medicine and Health Sciences
ISSN: 2517-9969
Vol:4, No:9, 2010

Shannon-Weaver Biodiversity of Neutrophils in Fractal Networks of Immunofluorescence for Medical Diagnostics

N.E.Galich

Abstract**—**We develop new nonlinear methods of immunofluorescence analysis for a sensitive technology of respiratory burst reaction of DNA fluorescence due to oxidative activity in the peripheral blood neutrophils. Histograms in flow cytometry experiments represent a fluorescence flashes frequency as functions of fluorescence intensity. We used the Shannon-Weaver index for definition of neutrophils' biodiversity and Hurst index for definition of fractal's correlations in immunofluorescence for different donors, as the basic quantitative criteria for medical diagnostics of health status. We analyze frequencies of flashes, information, Shannon entropies and their fractals in immunofluorescence networks due to reduction of histogram range. We found the number of simplest universal correlations for biodiversity, information and Hurst index in diagnostics and classification of pathologies for wide spectra of diseases. In addition is determined the clear criterion of a common immunity and human health status in a form of yes/no answers type. These answers based on peculiarities of information in immunofluorescence networks and biodiversity of neutrophils. Experimental data analysis has shown the existence of homeostasis for information entropy in oxidative activity of DNA in neutrophil nuclei for all donors.

Keywords**—**blood and cells fluorescence in diagnostics of diseases, cytometric histograms, entropy and information in fractal networks of oxidative activity of DNA, long-range chromosomal correlations in living cells.

I. Introduction

1. Neutrophils are the important components of the immune system. Immunity is connected with metabolic, geographical, ecological, information, genetical and migration networks of diverse populations of neutrophils in the human body. The nature of most of these networks is unknown. We observed new features of oxidative activity networks in neutrophils' populations. We investigate the experimental data of DNA fluorescence in neutrophils nuclei of peripheral blood. DNA fluorescence is triggered by biochemical reactions of respiratory oxidative burst [1-3]. Oxidative activity of DNA is very important for aerobic organisms. Oxidative activity burst is visualized in fluorescence. Fluorescence statistics are presented in histograms. Immunofluorescence histograms are obtained by flow cytometry method [4]. The method is based on registrations of large collections of photon count statistics for fluorescence cells, DNA and RNA. The measurement is performed at thousands cells per second rates. Flow cytometry is a unique method for analysis of gene regulation, gene expression and their correlations in live population of cells.

2. Spatial resolution of the instrument in flow cytometry may be very high. This fact is little known and poorly used. Resolution and sensibility of the instrument in flow cytometry measurement allows registering very small heterogeneities of neutrophils, with dimensions of the order of nanometers and smaller sizes, inaccessible of optical microscopy. Registration of typical fluorescence flash with duration $\sim 10^{-9}$ s in the flow of blood flowing through the laser beam with the velocity ~1 m/s provides measurement with spatial scales $\sim 10^{-9}$ m. Synchronization and registration of short fronts $\sim 10^{-12}$ s of fluorescence pulses gives an increasing of sensitivity and extending of lower limit of measurements in the flow direction. Registration of very small heterogeneities allows detecting new peculiarities of neutrophils in flow cytometry. Diversity of neutrophils must be larger than can be seen in the optical microscope. Definition of diversity of fluorescent cells also depends on the gradations of glow brightness in registration of flashes' intensity. Number of gradations of glow brightness is determined by the number of channels for fluorescence intensity measurements. These dependencies also are discussed in this paper.

3. Neutrophils come into the blood from different parts of the body. Neutrophils belong to different generations and different populations living under different conditions. The inhabitants of the Earth also exist in a heterogeneous hierarchical system. Biodiversity of living beings on Earth decreases with the deterioration of the ecological situation. Neutrophils may to have the opposite trend. Diseases are accompanied by increasing of pathogenic factors, germs and bacteria. They affect on the immune system, immune response and on neutrophils in the organism. Neutrophils seek to participate in the fight against each infection. Therefore biodiversity of neutrophils in the blood may be increased with a deterioration of health, when increased the number of diseases or when increased the severity of the illness.

4. In this communication we analyze immunofluorescence characteristics in order to have quantitative criteria of general health status for clinical practice. These criteria can be interconnected with neutrophils' biodiversity. We can consider the human organism as an ecological system. Bad ecology is equivalent of a disease. Good conditions for environment in ecology reflect rich diversity for flora and fauna. Quantitative measure of quality in ecology is based on Shannon-Weaver index of biodiversity [5,6]. Main interest is focused on the definition of quantitative parameters of neutrophils' biodiversity in immunofluorescence. We used the

Author is with the Experimental Physics Department, Saint-.Petersburg State Polytechnic University, 195251, Saint-.Petersburg, Russia (e-mail: n.galich @ mail.ru).

Shannon-Weaver index for definition of neutrophils' biodiversity and Hurst index [7] for definition of fractal's correlations in immunofluorescence, as the basic quantitative criteria. Irregular nature of immunofluorescece and fractals in fluorescence networks closely connected with genes' expression [8].

We analyze Shannon-Weaver biodiversity and Hurst index for frequency distributions of immunofluorescence, for frequency distributions of information and information entropies of fluorescence under different histograms' ranges or under different fluorescence networks' scales. So we have spectra of different fluorescence networks and spectra of Shannon-Weaver biodiversity and Hurst index in these networks for each donor.

5. Each experiment for each individual donor gives correlations and statistical features of fluorescence for tens of thousands of young and old neutrophils in one cytometric histogram. These are no small statistics. Non-Gaussian exponential growth of central moments $M(i,k)$ of fluorescence intensity fluctuations i causes strong difficulties of experimental results analysis [2]. Statistical instabilities of local fluorescence intensity distributions are the main reason of difficulties. Three typical histograms are shown in Fig.1 [8].

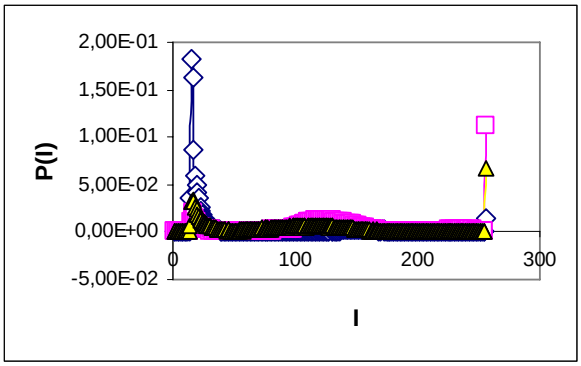

Fig. 1 Dependence of spontaneous fluorescence flashes number $P(I(256))$ on their intensity $I(256)$, non-dimensional variables; area under the final histograms normalized to unit; rhomb points correspond to bronchial asthma. Total number of flashes is $N_0 = 76623$; quadrate points correspond to healthy donor. Common number of flashes is $N_0 = 40109$; triangle points correspond to oncology disease. Common number of flashes is $N_0 = 40752$ .Common number of channels for fluorescence intensity $I(256)$ measurements is 256

Average value of intensity is smallest than dispersion for all of histograms. Dispersion of intensity is smallest than asymmetry and others higher statistical moments of intensity fluctuations, as it is shown in Fig.2 for any histograms of iommunofluorescence. Therefore standard statistical methods failed.

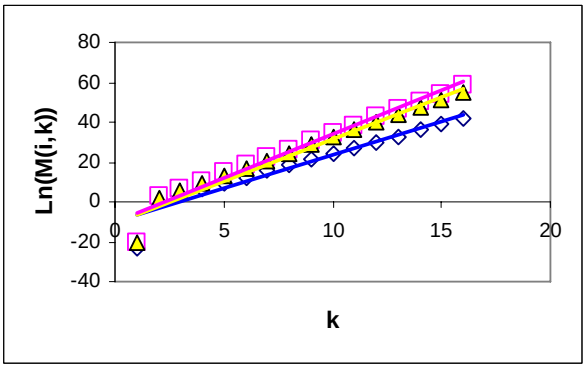

Fig. 2 Logarithmic distributions of intensity central moments $LnM(i,k)$ as function of moment's number k, for histograms in Fig.1; $< i^k >= \sum_{l=1}^{l=256} i^k \times P_l = M(i,k)$. Details are described in [8].

6. We develop a sequence of new nonlinear statistical methods to data analysis of immunofluorescence. Now we analyze evolution of different average values of immunofluorescence parameters with changes of columns in histograms and with variations of scales and of ranges for distributions of frequencies of flashes, information and information entropies.

We have many of meaningful information about condition of DNA in immunofluorescence histograms. Fragments of nuclear and mitochondrial DNA with oxidizing metabolism activity and oxidants determine the basic place for localization of the fluorescent dye [1-4,8,9]. Localization and distribution of fluorescence dye determine the intensity and statistics of fluorescence. The heterogeneous fluorescence of chromosomes reflects simultaneously the genetic special, individual features and immune response to the pathogenic actions.

We analyze Shannon entropies and fractals of immunofluorescence networks in order to found the simplest universal correlations for clear diagnostics of pathologies in wide spectra of diseases.

II. Preparations and Measurements of Fluorescence

We present new statistical treatment approaches of the highly sensitive quantitative method [2] for registration the inflammatory reactions of organism founded on collective cytofluorescence features. The method based on the flow cytometrical measurement of the capability of the peripheral blood neutrophils for the reaction of respiratory burst or oxidizing explosion [1,3].

Experimental methods and procedures are described in [2,8,10,11]. Experiments based on respiratory burst or oxidizing explosion [1,3]. The volume of peripheral blood is V = (1 ... 2) ml. We used hydroethidine addition with concentration 150 μg/ml for fluorescence initiation. Small concentration 100 *ng* /ml additives of phorbol myristate acetate (PMA) to blood samples ensure the intensive staining of the cell nuclei of polymorph nuclear leukocytes. At the beginning hydroethidine is transformed in ethidium bromide as the results of chemical oxidative reactions in the blood

cells. Ethidium bromide binds with fragments of nuclear DNA and has strong red fluorescence excited by TEM_{00} mode radiation Argon laser light at 488 nm wavelengths. Intercalation of ethidium bromide in chromosome is determined by oxidative activity fragments of DNA. Fluorescence reflects the ability of cell to produce oxygen radicals, i.e. the respiratory burst activity. Details of experimental procedures, preparations and tests are described in [8,10,11]. The rate of measurements is about $(1\text{-}2)10^4$ cells per min. Mean time of the measurement of one model is about 2 min. This empirically selected regime is self-consistent with noises level of various nature [10] and gives statistically stable and reproducible results. The inaccuracy and reproducibility for preparations and measurements procedures usually compose $\approx 2\%$. This inaccuracy and reproducibility level corresponds to unavoidable and irremovable noises and errors both physical and biological nature [10].

Results are represented in the form of immunofluorescence histograms as dependence the number of flashes on intensity of flashes for 256 channels of intensity measurements (see Fig.1). Typical common number of flashes is $N_0 \sim 10^4 \ldots 10^5$. Ranges of intensities I vary from 1….14 to 256 dimensionless units. These ranges of I correspond to numbers of channels l for intensity measurements. Low boundary of intensities range $I_{low} \sim 12$ usually constitutes 12 and in the general case is variable. The fluorescence with intensity less than lowest boundary is not considered. Lowest boundaries of intensities are limited by means of discriminator for interception of background noise. Background noise is cut off. Three typical examples of histograms are shown in Fig.1.

III. Information and Shannon Entropy for Distributions of Flashes; Biodiversity

We use centered random variables and their centered moments. This approach is necessary to the exception the uncontrollable and systematic errors, instabilities of algorithmic procedures and corresponding drift of averages.
Let us consider the relative deflections of fluorescence flashes number from their average level

$$n = (P_l - < P >) = < P > \times (\frac{N}{< N >} - 1), \quad (1)$$

$< P >= (I_{\max} - I_{\min})^{-1}$, $N = N(l)$,
$< N >= N_0 \times < P >$, $P_l = N(l) / N_0$, $l = 1,2,...256$,
where symbol $< \ldots >$ denotes statistical average of the fluorescence fluctuations for all 256 channels of intensity measurement ; measurement ; $P_l = N(l) / N_0$ is the probability distribution density of the flashes number ; $N = N(l)$ is the number of flashes with the assigned intensity $I = l$ for the dimensionless intensity I coincides with the number of channels l ; N_0 is common number of flashes; average value of flashes number is $< N >= N_0 \times < P >$. Mean probability value is $< P >= (I_{\max} - I_{\min})^{-1} = 1/256$.

Central moment $M(n,k)$ for relative fluctuations of flashes number n are defined as statistical average $< n^k >= M(n,k)$, where k determines the order of moment $M(n,k)$, symbol $< \ldots >$ denotes statistical average for fluorescence fluctuations.

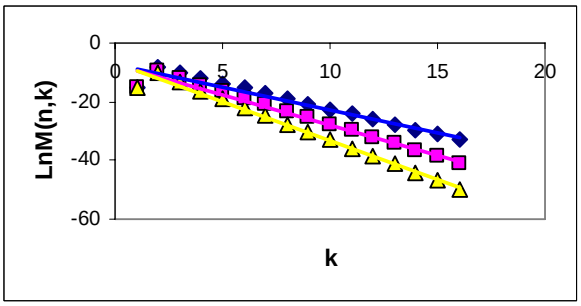

Fig. 3 Dependence of logarithm of central moments $< n^k >= M(n,k)$ on moment's number k for histograms in Fig.1

Rates of decreasing of $M(n,k)$ with growth of k are different for different health statuses. We have the exponential growth of central moments for intensity $i(l) = (I \times P_l / < I > -1)$, $< i^k >= \sum_{l=1}^{l=256} i^k \times P_l = M(i,k)$ in Fig.2. This is equivalent of the statistical instability for local intensity distributions. We have the exponential decreasing of central moments $M(n,k)$, if k>2, in Fig.3. Therefore, distributions of relative value of the number of flashes may to have a probabilistic measure. Therefore function $P_l = N(l) / N_0$ can be considered as density of probability for number of flashes. Then we can enter the information for the distribution of flashes

$$J_l = -LnP_l \quad (2)$$

Information entropy $S(P)$ for the distribution of the number of flashes P_l has the form

$$S(P(I(256)) = < J_l >= -\sum_{l=1}^{l=256} P_l \times LnP_l \quad (3)$$

Shannon entropy (3) is defined by the probability distribution of fluorescence flashes P_l in l' channels for intensity measurements. Information (2) is defined by the probability of occurrence the fluorescence flash of neutrophil with specified intensity. Thus, immunofluorescence histogram visualizes the probability of occurrence of neutrophils with a specific oxidative activity. Therefore, Shannon entropy also characterizes the Shannon-Weaver index $S(P)$ [5,6] for the biological diversity of neutrophils. Distinctive features of neutrophils here are determined by different oxidative activities of DNA. Distinctions in neutrophil activity for oxygen metabolism interconnected with peculiarities of chromosomes structure and chromosomal correlations in nucleus of neutrophils. These correlations are reflected

networks of ethidium bromide in chromosomes due to oxidative activity of DNA.

IV. Changes of Information and Entropy with Reduction of Histogram's Range

How will be changing the information due to reduction of histogram's range? Let us introduce integer R as the upper limit for the number of channels l=I during reduction of histogram's range. Integers R define the total histogram range for every reduction of common number of histogram's columns. Then we obtain the dependence of the total information J

$$J(P((R),R)=\sum_{m=1}^{m=R} J_m\,,\quad J_m=-LnP_m \qquad (4)$$

on R (see Fig.7). Changes of Shannon entropy $S(P(R),R)$ due to reduction of range R is described by the ratio

$$S(P((R),R)=\sum_{m=1}^{m=R} S_m(P_m)\,,\ S_m(P_m)=-P_m\times LnP_m \qquad (5)$$

where probability density due to reduction of range R is $P_m=N(m)/N_R$,number N_R characterize total number of flashes in reduced histograms. Reduced total number of flashes N_R is defined by the condition that $\sum_{m=1}^{m=R} P_m=1$. Dependence of N_R on R is linear and $N_R=N_0\times(R/256)$. Shannon entropy $S(P(R),R)$ describes the Shannon-Waver index of biodiversity [5,6] for different range R (see Fig.8).

Let us consider reduction of histogram's ranges. Normalized frequency P_m and frequencies J_m, S_m change due to reduction of R as it shown in Figs.4, 5, 6 for distributions of flashes P_m, information J_m and entropy S_m.

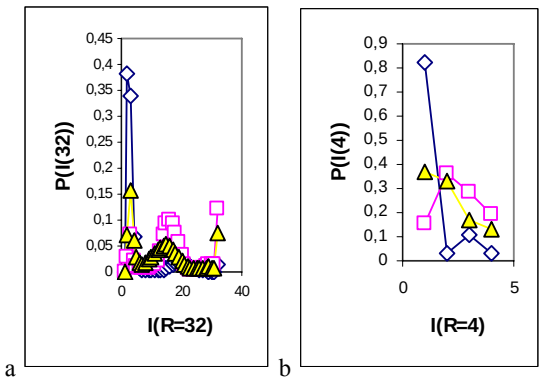

Fig. 4 Dependence of normalized spontaneous fluorescence flashes frequency P_m on intensity I; (a) histogram range R=32 (b) histogram range R=4; initial histograms see in Fig.1

Here reductions of histogram's range have analogies with averaged measurements and with decreasing the number of channels for measurements of fluorescence. Contribution of various-scale noise due to transition to large-scale histograms can be extraordinarily large and have a different, both positive and negative sign in the distribution of columns in final low-range histograms, as shown in Figs.4b, 5b and 6b.

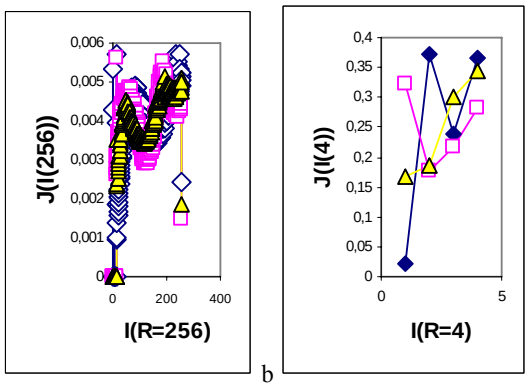

Fig. 5 Dependence of information frequency $J_m=-LnP_m$ on intensity I; (a) histogram range R=256 (b) histogram range R=4; initial histograms see in Fig.1

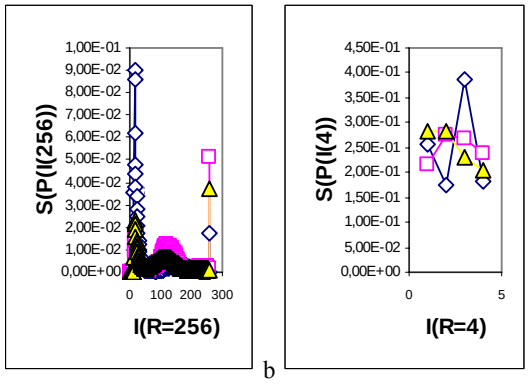

Fig. 6 Dependence of entropy frequency S_m on intensity I; (a) histogram range R=256 (b) histogram range R=4; initial histograms see in Fig.1

We observe qualitative changes for distributions of frequencies P_m, J_m, S_m due to reduction of histogram's range in Figs.4, 5, 6. Changes in low range (R=4) distributions for different health status in Figs.4, 5, 6, are very radical, in the contrast of qualitative similarity of different initial histograms in Fig.1 (R=256). We observe very strong stratification for short range (R=4) in the contrast from high range (R=256) distributions in the space of intensity. What it means for information about biodiversity?

Low range (R=4) distributions in Figs.4b, 5b and 6b give approximately concave and convex parabolas for different health status. Very clear qualitative difference in health status are reflected in the qualitative difference of concave/convex parabola for each of distribution of all frequencies P_m, J_m, S_m , when range R=4 [11,12]. Concave parabola P(I(4)) corresponds to inflammations. Convex parabola P(I4)) corresponds to healthy people. Parabola with zero curvatures corresponds to autoimmune diseases. Preliminary results of

analysis of low range histograms and bifurcations of immunofluorescence distributions were discussed in [11,12]. This classification allows dividing any sets of histograms on three big groups for various health statuses and for different classes of diseases. We observed the inflammatory processes after different surgical interventions, appearance and flow of autoimmune processes with the post infection complications, neurological and heart complications after diphtheria, chronic inflammation with rheumatoid arthritis, inflammatory reaction with bronchial asthma, course of inflammatory events with the myocardial infarctions, inflammations with system lupus erythematosis, hepatitis, peritonitis, purulent appendicitis, pneumonias, cardiovascular, oncology and other diseases. Some illustrations of this approach to diagnostics for the disturbance of oxidizing metabolism are shown in Fig.14,15.

More valuable results are based on the dependence of total parameters J, S on histogram's range R in Fig.7, 8. These correlations give very versatile and precision tools for analyze the change of biodiversity and information at change of R. These correlations have of greatest interest for quantities' diagnostics of health status and types of illness (see parts 5, 8).

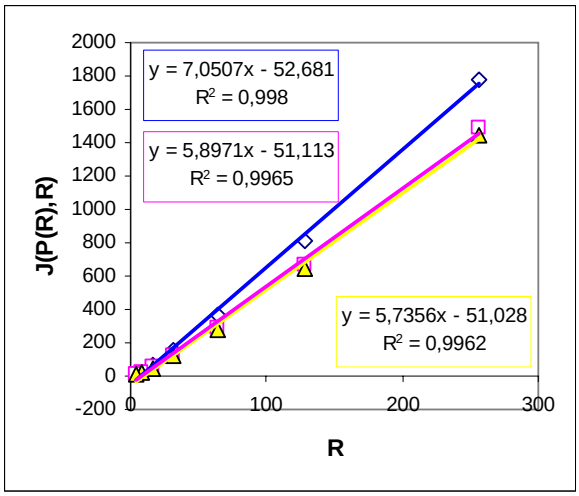

Fig.7 Dependence of information $J(P(R),R)$ on range of histogram R; initial histograms see in Fig.1

Dependence of information $J(P(R),R)$ on R is linear and has different rates for different health status. Stratifications of $J(P(R),R)$ for different diseases have the linear growth with increasing of R. Therefore we have a linear growth of diagnostic sensitivity of information with increasing of channels number.

We can expect a much more noticeable difference in the information $J(P(R),R)$ of histograms reaching a difference of 300% for 4096 channels measuring the intensity, instead of 20% for 256 channels as in Fig.7. Increasing of a difference in the biodiversity of neutrophils with growth of R for various diseases is not so strong.

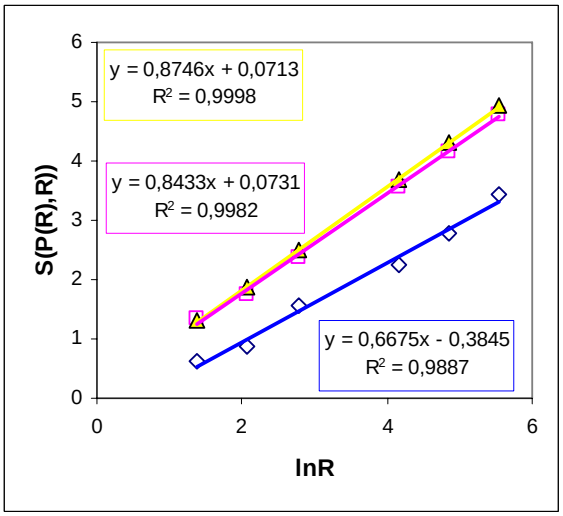

Fig. 8 Dependence of Shannon-Weaver index $S(P(R),R)$ for flashes distribution P_m of immunofluorescence on logarithm of range R; initial histograms see in Fig.1

We observe richer biodiversity of neutrophils for oncology and poorer biodiversity for inflammatory disease in Fig.8. Difference in the Shannon-Weaver index for oncology and for asthma combined $\approx$ 70% when R=256.

We have a logarithmic growth of diagnostic sensitivity of Shannon-Weaver biodiversity $S(P(R),R)$ with increasing of channels number R.

V. Hurst Index for Networks of Flashes in Immunofluorescence

Let us consider, briefly, fractal features of immunofluorescence for networks of flashes. Let us compare the brokenness for three typical histograms in Fig.1, using the Hurst exponent. Results are shown in Figs. 9.

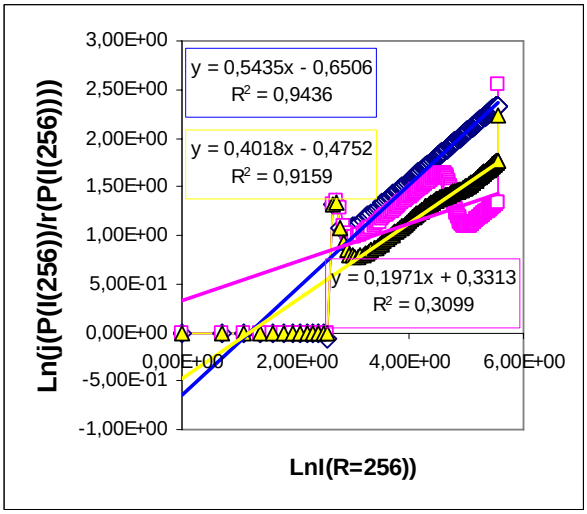

a

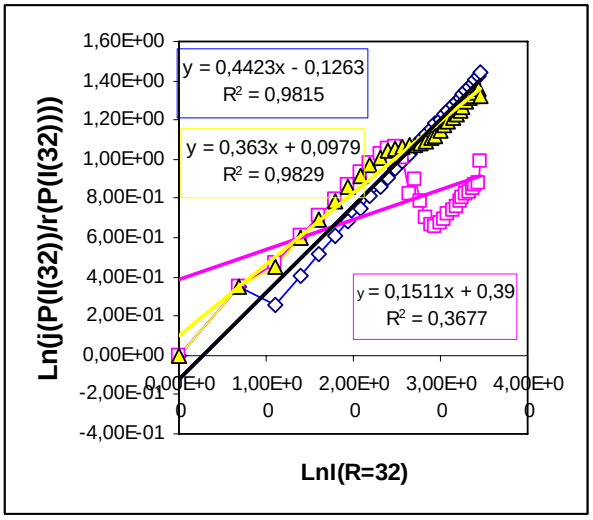

b

Fig. 9 Total Hurst exponent $H(P(R),(R))$ (a) Hurst exponent $H(P(I(256)) = \partial Ln(j/r)/\partial LnI$ for R=256; initial histograms see in Fig.1 (b) Hurst exponents $H(P(I(32)) = \partial Ln(j/r)/\partial LnI$ for R=32; initial histograms see in Fig.4a

Hurst exponent H_H [7] is determined by means of regression equation

$$Ln(j/r) = H \times LnI + const \quad (6)$$

where (j/r) is rescaled range ($r = j$), j is range or maximal deviation of $P(I)$ from local mean level, r is standard deviation of $P(I)$. Hurst index $H(P(R),R)$ for frequency of flashes P_m corresponds to fractal (Hausdorff) dimension D_H [7] if

$$D_H = 2 - H \quad (7)$$

In particular, the H exponent indicates persistent or correlated (H > ½) and anti-persistent or uncorrelated (H < ½) behavior of trend. Persistent behaviors are observed in Fig.9a for asthma, when H(R=256)=0.5435. Anti-persistent behaviors H(R=256)=0.1971 for healthy person and H(R=256)=0.4018 for oncology. Correspondence fractal dimensions are 1,4< D_H <1,8. We have different Hurst exponent for different three groups of diseases. Therefore, fractal structures and fractal dimensions of fluorescence networks depend on health status.

Reduction of histogram's range from R=256 in Fig.9a to R=32 in Fig.9b, shown changes of Hurst exponents. It means that we have different transformations of fractal networks for various health statuses with reductions of range. In Fig.9b we have only anti-persistent behaviors of H(R=32)<1/2 for any health status. Hurst index H(R=32) also depend on health status. More detail pictures about transformations of Hurst index due to reduction of range are shown in Figs.10.

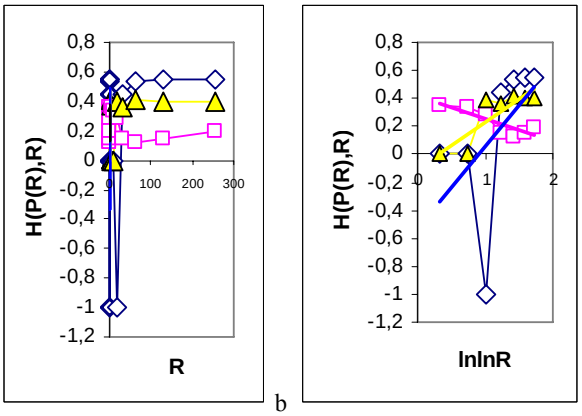

a b

Fig.10 Dependence of Hurst index $H(P(R),R)$ on range R (a) linear scales (b) double logarithmic scales; initial histograms see in Fig.1

We observe changes of hierarchy in Hurst exponents or in fractal dimensions of immunofluorescence for different range of networks. Good health corresponds to anti-persistent behavior of H<1/2 for any range number R. Unhealthy people corresponds to persistent behavior of H>1/2 for range number R> 64. From this point of view the dominant of anti-persistent immune behavior for healthy people gives richer spectra responses of immunity than more poor reaction of unhealthy people.

Dynamics of changes for Hurst exponents $H(P(R),R)$ with reduction of histogram's ranges R can give very clear criterion for estimation of health. Let us consider dependence of Hurst exponent H on double logarithm of range lnlnR in Fig.10b. We observe qualitative changes of trend of Hurst index distributions for healthy and unhealthy people in Fig.10b. We have the negative trend of H for good health and the positive trend for illness with the increasing of R, i.e. we have opposite trends in the evolutions of immunofluorescence networks with different ranges for health and for illness.

Details of oxidative activity of DNA for nets of bridges, percolations and correlations between flashes in their interconnections with local placements in chromosomes are unknown. Different assumptions can to lead to regressions as in Fig.10b. For instance, linear regressions in Fig.10b are the same linear regressions in [13] (see Fig.5 in [13]) for combined networks of metabolism, interaction, regulation and expression in a particular for composite motifs in the design of molecular networks. More general reason of positive and negative trends in Fig.10b may be connected with peculiarities of information dynamics in large scale networked systems (see true and false distributions in [14]).

Actually, we determine the clear criterion of a common immunity and human health status in a form of yes/no answers type. Negative sign of trend in the dependence H(R) on R in double logarithmic scale lnlnR in Fig.10b is equivalent of health. In opposite trend we observe different diseases. These simplest answers give the structural changes of immunofluorescence networks with different ranges.

Here reductions of histogram's range have analogies with averaged measurements and with decreasing the number of channels of measurements. Changes in low range distributions

(R=4) with variations of health status in Figs.4, 5, 6, are much more radical than changes in initial histograms in Fig.1 for bigger range (R=256). Radical changes in low range distributions (R=4) for different health status depend on a brokenness and irregularity of histograms. Peculiarities of long-range correlations and properties of immunofluorescence noise are described in [9]. Contribution of noise in large-scale histograms, with R=4, can be extraordinarily large. This contribution gives positive and negative curvatures for approximations of frequency distributions P_m in histograms (see Fig.14b,15b). We have different structures of large-scale's and small-scale's noises [9]. Therefore we have different structures of large-scale and small-scale immunofluorescence networks. This is reflected in the change of magnitude and character of Hurst exponents in averaged distributions of fluorescence, with different scales of averaging in Fig.10. Here Hurst exponents characterize fractal brokenness of histograms and fractal structure of immunofluorescence networks.

We have different Hurst exponents for frequencies of flashes P_m, information J_m and Shannon-Weaver index S_m. These differences reflect peculiarities of variations in the structure of networks for flashes, information and entropy.

VI. Hurst Index for Networks of Information Entropy in Immunofluorescence

Let us consider, briefly, fractal features of immunofluorescence for networks of information entropy. Let us compare the brokenness for three typical histograms in Fig.1, using the Hurst exponent. Results are shown in Figs. 11.

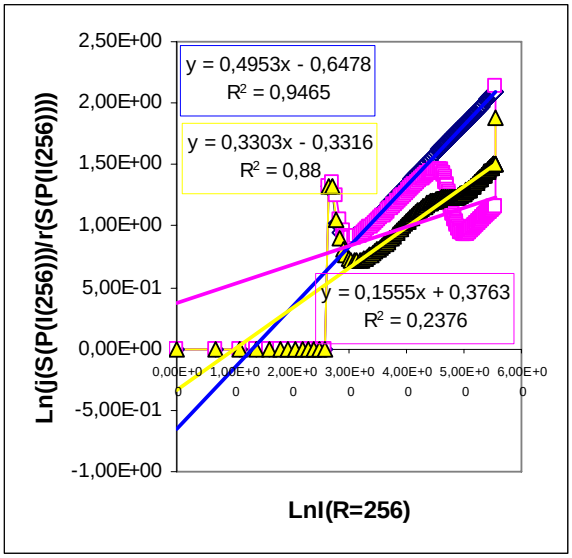

Fig.11 Total Hurst exponent $H(S(P(R)),R)$ Hurst exponent for range R=256; initial histograms see in Fig.6a

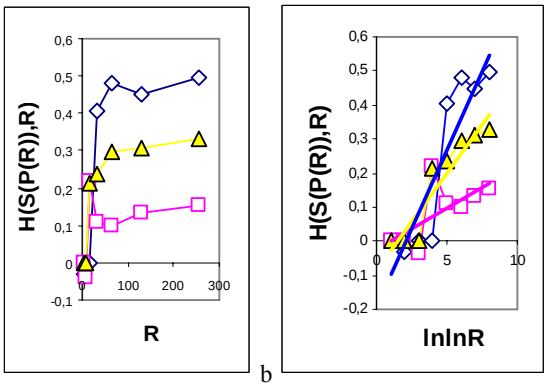

a b

Fig.12 Dependence of Hurst index $H(S(P(R)),R)$ on range R (a) linear scales (b) double logarithmic scales; initial histograms see in Fig.6a

Hurst index $H(S(P(R)),R)$ for frequency distribution of entropy S_m corresponds to fractal (Hausdorff) dimension D_H(H(S(P(R),R) in Eqn. (7). Differences between peculiarities in Fig.10 and Fig.12 reflect differences between fractal peculiarities of networks for P_m and for S_m.

We observe only anti-persistent behavior of Hurst exponents for entropy distributions $H(S(P(R)),R)$ in Figs.11,12 for any health status in the contrast from Hurst exponents for flashes distributions $H(P(R),R)$ in Figs.9,10. We observe more uncorrelated behavior of information entropy fluctuations than fluctuations of flashes number, i.e. $H(S(P(R)),R) < H(P(R),R)$ for any health status. Finally, we have unchangeable sign of trends in the dependencies of $H(S(P(R)),R)$ on $\ln\ln R$ in Fig.12. Therefore, fractal structure of entropy networks is more conservative than structure of networks for flashes when is changed a state of health.

Ratio of Hurst index (H(S(P(R),R) for asthma H(S,asthma) is more than Hurst index for oncology H(S,oncology) and more than Hurst index H(S, healthy) for healthy man. Ratio H(S,asthma)/ H(S,healthy) is close to 5. Ratio H(S,asthma)/ H(S,healthy) is close to 3. These ratios are rather stable when R>64.Thus, the fractal structure of frequency distributions of Shannon-Weaver biodiversity S_m has noticeable and stable stratifications for different health statuses. These stratifications give a clear estimation of differ between different health statuses and illnesses.

VII. Empirical Invariants for Information Entropy in Oxidative Activity of DNA in Neutrophils

For stability living of human and animal is required homeostasis. For example, a healthy human characterizes homeostasis in the body temperature, heart rate and other parameters. Is it possible to define a homeostasis of oxidative activity of DNA? Is it possible to define the invariant for the Shannon-Weaver index? In other words, what manifestations of activity of DNA can give the identical conditions of life for all of neutrophils, for any people? When, under what

circumstances, Shannon-Weaver index may to have practically the same value for neutrophils of all living persons, regardless of health status? For what parameters observed biological monotony? This question interconnected with the fact that belonging to the human species is not dependent on nationality, age, gender and geography. All people breathe air. We are aerobic organisms. Is there anything similar to the homeostasis in the oxidative activity of DNA? Let us change the probabilistic measure in the determination of Shannon entropy. Let us introduce entropy $S(J(R),R)$ for probability distribution of information

$$S(J(R),R)=\sum_{m=1}^{m=R} S_m(J^n{}_m)\,,\; S_m(J^n{}_m)=-J^n{}_m\times Ln(J^n{}_m) \quad (8)$$

where $J^n{}_m$ defines normalized distribution for flashes of information

$$J^n{}_m=J_m(P_m)/J(P(R),R)\,,\; J(P(R),R)=\sum_{m=1}^{m=R} J_m(P_m) \quad (9)$$

We observe the universality of $S(J(R),R)$ in Fig.13.

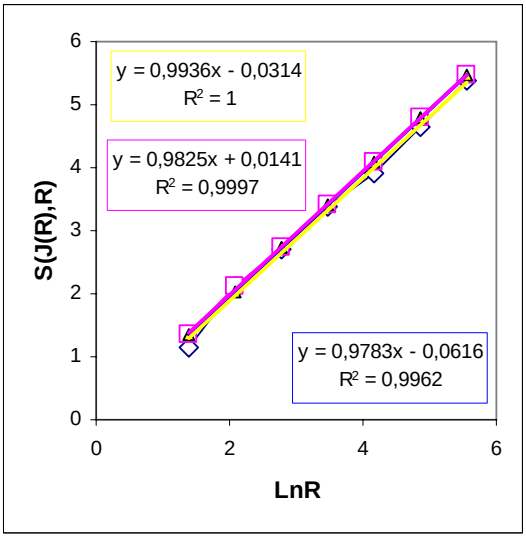

Fig.13 Dependence of Shannon-Weaver index $S(J(R),R)$ for information distribution $J^n{}_m$ of immunofluorescence on logarithm of range R; initial histograms see in Fig.1

In Fig.13 we observe invariance in identical dependencies of entropy on range R for any state of health and for different people. Coincidence is not absolutely perfect and is determined by experimental errors ~ 2% .We have such a coincidence for all patients (see also part 8). May be this a clear sign of homeostasis in oxidant activity of DNA in living cells for all living people?

VIII. Experience and Applications in Treatment and in Natural Conditions

Preliminary experiments had shown the usage opportunities of proposed approach for the solution of various medical problems (see part 4 and [9]).

We analyzed wide spectrum of different inflammatory and autoimmune diseases, which include several ten designations. Analysis of immunofluorescence histograms shows the cases previously undetected diseases.

Let us consider examples of proposed criteria for control of health status in medical treatment and in natural conditions.

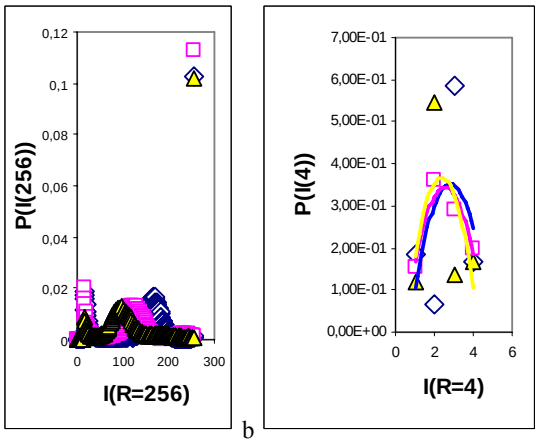

Fig.14 Dependence of normalized spontaneous fluorescence flashes frequency $P(I(R))$ on intensity $I(R)$, for one, invariably healthy, donor at different times. Rhomb points correspond to the total flashes number $N_0=30832$, analysis time is 19 July (first year); triangle points correspond to the total flashes number $N_0=38758$, analysis time is 11 July (next year); square points correspond to the total flashes number $N_0=40109$,analysis time is 03 June, before 11 July (a) histogram range $R=256$ (b) histogram range $R=4$, initial histograms see in Fig.14a

We observe rather stable character of distributions for frequencies of flashes P_m in Fig.14b. It means stability of immunity for given healthy donor during one year.

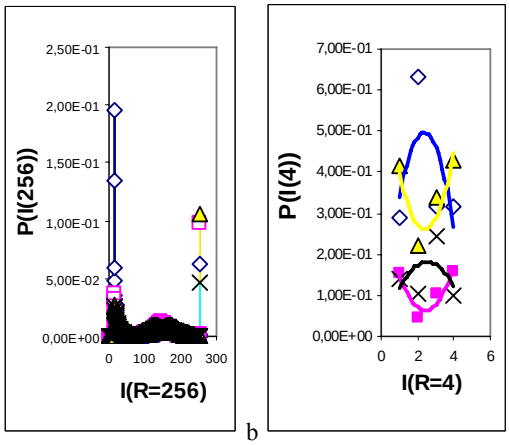

Fig.15 Dependence of normalized spontaneous fluorescence flashes frequency $P(I(R))$ on intensity $I(R)$, for one donor with oncology disease; symbol rhomb relates to analysis date 05 November, N_0=43752; symbol quadrate corresponds to 15 December, after treatment of hepatitis B, N_0=26265; triangle points correspond to N_0=45142, analysis time is 21 March next year; cross-points correspond to the total number of flashes N_0=45981, analysis time is 11 July next year, after trying the treatment of oncology diseases (a) histogram range $R=256$ (b) histogram range $R=4$, initial histograms see in Fig.15a

Let us examine some example in Figs.15 for oncology sick. In the medical treatment process the patient was infected by hepatitis B. Standard medical treatment against the hepatitis leads to decreasing of inflammation, i.e. common number of flashes N_0=43752 down to N_0=26265. In Fig.15b approximation's distribution P_m of concave parabola for rhomb points transforms to convex parabola for quadrate points. Concave parabola characterizes an inflammation [11,12]. This means the dominant of hepatitis, while standard biochemical tests have shown that hepatitis suppressed. Further degradation of the patient's health leads to concave parabola for triangle points in Fig.15b. Next medical treatment is described the convex parabola for cross-points in Fig.15b. We have a complex combination of incurable diseases of inflammatory and autoimmune nature. Sequential treatment of only one disease leads to deterioration in the presence of a second disease. Convex/concave parabolas in Fig.15b describe stability/instability of immune responses [12]. A quantitative description of histograms for information $J(R)$, information entropies and Hurst indices is shown in Fig.16-19.

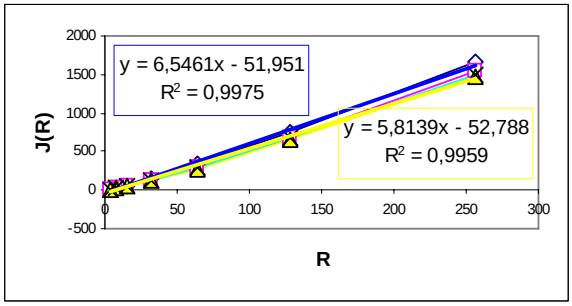

Fig.16 Dependence of information $J(P(R),R)$ on range of histogram R; initial histograms see in Fig.15; variability in oncology

We observe variations of $J(P(R),R)$ during treatments of oncology and hepatitis for the sequence of events in Fig.15. Comparisons of Figs. 16 and 7 show the range of modifications the information in the course of treatments.

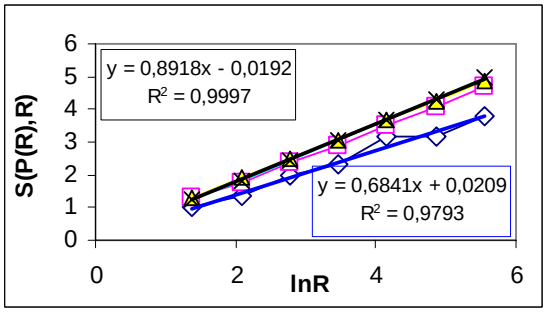

Fig. 17 Dependence of Shannon-Weaver index $S(P(R),R)$ for flashes distribution P_m of immunofluorescence on logarithm of range R; initial histograms see in Fig.15; variability in oncology

We observe stratifications of Shannon-Weaver index $S(J(R),R)$ during treatments of oncology and hepatitis for the sequence of events in Fig.15. These stratifications reflect the sensitivity of registration of quantitative changes in DNA oxidative activity for neutrophils' populations during medical treatments. Actually, it is hopelessly ill person as can be seen from constantly of positive sign of trends to increasing of Hurst indices in Fig. 18.

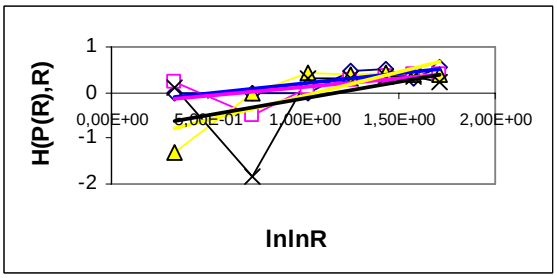

Fig.18 Dependence of Hurst index $H(P(R),R)$ on range R in the double logarithmic scale; oncology, initial histograms see in Fig.15a

We observe positive trends of Hurst index $H(P(R),R)$ and slight variations of these trends in Fig18. Comparisons of Figs. 18 and 10b show the range of modifications of positive trends during medical treatments. Constantly of positive sign of trends means fluctuations of health states in the frame of continuing incurable illnesses for this case of oncology and hepatitis.

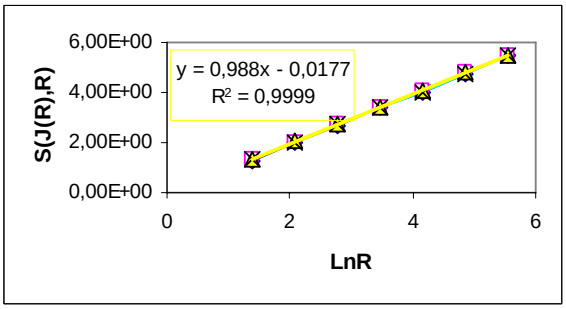

Fig.19 Dependence of Shannon-Weaver index $S(J(R),R)$ for information distribution $J^0{}_m$ of immunofluorescence on logarithm of range R; initial histograms see in Fig.15; variability in oncology

We observe of invariants of $S(J(R),R)$ during treatments of oncology and hepatitis for the sequence of events in Fig.15. We observe the same pictures in Fig.13,10 for different donors and in Fig.20 for healthy donor.

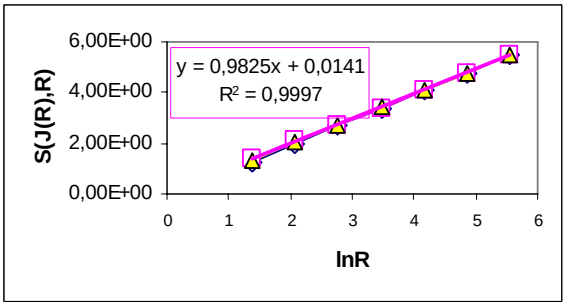

Fig. 20 Dependence of Shannon-Weaver index $S(J(R),R)$ for information distribution $J^0{}_m$ of immunofluorescence on logarithm of range R; initial histograms see in Fig.14; variability in good health

We have coincides of Shannon-Weaver indices S(J(R),R) for information $J^0{}_m$ in Fig.13,19,20 for any donors with any

health status. Therefore, we observe invariant of S(J(R),R) for any neutrophils' populations and for all living people.

Others correlations for histograms of healthy donor are shown in Fig.21-23.

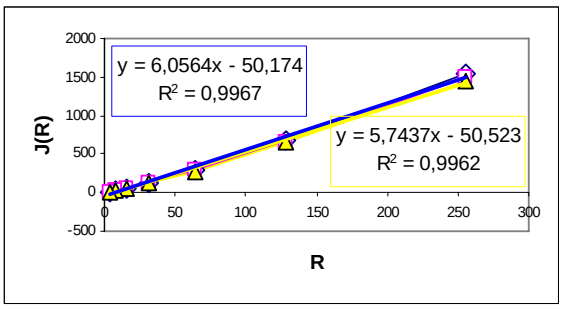

Fig. 21 Dependence of information $J(P(R),R)$ on range of histogram R; initial histograms see in Fig.14; variability in good health

We observe no strong variations of $J(P(R),R)$ for healthy person for the sequence of events in Fig.14. We observed differences in the rate of trends in Fig.7, Fig.16 for oncology and hepatitis during treatments and in Fig.21 for healthy donor in natural conditions.

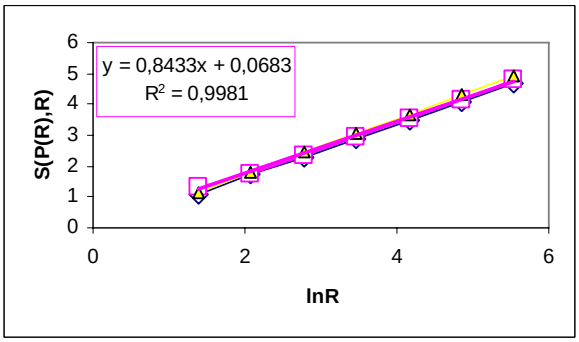

Fig. 22 Dependence of Shannon-Weaver index $S(P(R),R)$ for flashes distribution P_m of immunofluorescence on logarithm of range R; initial histograms see in Fig.14; variability in good health

Variations of Shannon-Weaver index S(P(R),R) for healthy donor in Fig.22, for the sequence of events in Fig.14, are practically neglectable. Good immune system of this healthy donor gives constantly stable populations of neutrophils.

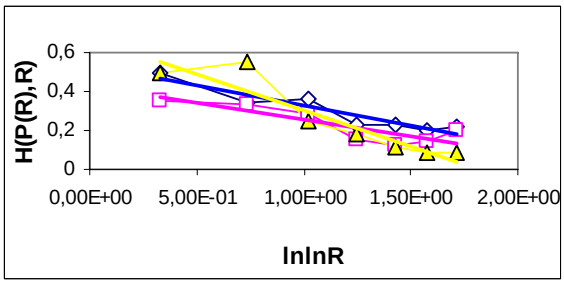

Fig. 23 Dependence of Hurst index $H(P(R),R)$ on range R in the double logarithmic scale; healthy donor, initial histograms see in Fig.14a

We observe negative trends and slight variations of these trends in Fig23. Comparisons of Figs.23 and 10b show the range of modifications of negative trends for healthy donor. Constantly of negative sign of trends means fluctuations of health states in the frame of continuing good health.

Dependencies of Hurst index $H(P(R),R)$ on range R for healthy and unhealthy donors in Figs.23 and 18 are the same dependencies in Fig.10a for different health statuses.

Only two types of regressions for Hurst indices $H(P(R),R)$ with positive and negative trends as in Fig.10b have observed in double logarithmic scales lnlnR for any donors. Positive trends in Fig.18 are typical for illness. Negative trends in Fig.23 are typical for health. Therefore, increasing or decreasing of fractal dimensions of immunofluorescence networks due to range reduction gives clear answer about general health status of donor. This manifests the role of multifractal structures in the organization of networks' hierarchy for oxidative metabolism and for health. First type of hierarchy networks of flashes corresponds to increasing of Hausdorff dimension $D_H = 2 - H$ with growth of R in Fig.23 for healthy donor. Second type of hierarchy networks of flashes corresponds to decreasing of Hausdorff dimension $D_H = 2 - H$ with growth of R in Fig.18 for oncology and hepatitis. In the last case we observe a negative Hurst index or abnormal $D_H > 2$ if $R < 16$; these situations interconnected with bad self feeling. The same abnormal Hausdorff dimension $D_H > 2$ we observe in Fig.10 for bronchial asthma.

We observe noticeable changes for distributions of Shannon-Weaver index of biodiversity $S(P(R),R)$ due to reduction of histogram's range in Fig.17,18. This means essential changes of biodiversity of neutrophils in medical treatment of oncology and hepatitis. Stratification of dependencies $S(P(R),R)$ on R in Fig. 17 has shown that biodiversity can give very sensitive criterion for estimations of health status and variability of health. Slow variability of immunofluorescence networks for healthy donor, as shown in Figs.20-23, characterizes very stable immune system of given person with good health.

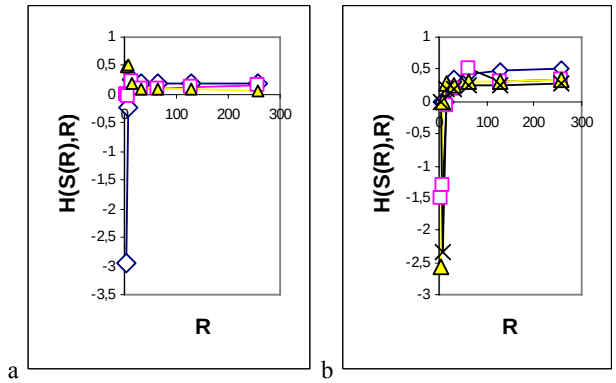

Fig. 24 Dependence of Hurst index $H(S(P(R)),R)$ on range R (a) healthy donor; initial histograms see in Fig.14a (b) oncology; initial histograms see in Fig.15a

Changeability of Hurst indices $H(S(P(R)),R)$ for frequencies of Shannon-Weaver index S_m in Fig.24a didn't has radical variations in natural condition during one year; donor with good health has stable networks of information entropy. Medical treatment of oncology and hepatitis brings more noticeable changes of Hurst indices $H(S(P(R)),R)$ in Fig.24b. Strong variations of $H(S(P(R)),R)$ for radical different health statuses in Fig.12a differ from changes of $H(S(P(R)),R)$ in Fig.24b. This means that medical treatments of oncology and hepatitis were not very successful. These treatments influenced on the positive change of immune response (see Fig.15b) and prolonged the life of donor.

IX. Conclusion

Flow cytometric measurements of respiratory burst manifest not only genomic features for alone DNA, but also the complete set of working chromosomes.

We have introduced various integrated parameters such as Shannon entropies and Hurst indices for information and fractal structures in immunofluorescence based on distributions of flashes P_m, information J_m and entropy S_m. Using of these integrated parameters are shown in Figs.4b,5b, 6b,7, 8, 10,12,14b,15b,16-18,21-24 for clear and sustainable statistical differences of immunofluorescence histograms in medical diagnostics.

In this work we have shown that structural changes in information networks due to range reduction for histograms of multi-channel measurements is a novel characteristic for information of multi-channel fluorescence distributions. For example, diagnostics of health or illness status are depending on sign of trend for changes of Hurst index $H(P(R),R)$ with histograms' range reduction, as it is shown in Figs.10b, 18, and 23. Therefore, we have the clear general criterion of a common health/illness status in a form of yes/no answers type.

Only two types of regressions for Hurst indices $H(P(R),R)$ with positive and negative trends as in Fig.10b have observed in double logarithmic scales lnlnR for any donors. Positive trends as in Fig.18 are typical for illness. Negative trends as in Fig.23 are typical for health. Therefore, increasing or decreasing of fractal dimensions of immunofluorescence networks due to range reduction gives clear answer about general health status of donor. This manifests the role of multifractal structures in the organization of networks' hierarchy for oxidative metabolism and for health. First type of hierarchy networks of flashes corresponds to increasing of Hausdorff dimension $D_H = 2 - H$ with growth of R in Figs.10b and 23for healthy donor. Second type of hierarchy networks of flashes corresponds to decreasing of Hausdorff dimension $D_H = 2 - H$ with growth of R in Figs.10b (asthma and oncology) and in Fig.18 (oncology and hepatitis) for any illness. In the last case we observe a negative Hurst index or abnormal Hausdorff dimension $D_H > 2$ if range $R < 16$; these situations interconnected with bad self-feeling.

We introduce information $J(R)$ and frequencies of information J_m for distributions of immunofluorescence. A quantitative description of information due to reduction of histograms' range R gives various regular trends of $J(R)$ for different health status as in Figs. 7, 16 and 21. Information $J(R)$ has stratification and variations of trends for different diseases. Information $J(R)$ has a linear growth with increasing the number of channels R as in Fig.7. We show that information $J(R)$ can give a regular criterion for estimations of health status and variability of health in natural conditions and in medical treatment as in Figs.16 and 21.

We introduce Shannon information entropy S for different probabilistic measure of immunofluorescence. Shannon entropy $S(P(R),R)$ for frequency of flashes P_m defines Shannon-Weaver index of biodiversity for neutrophils. Shannon-Weaver biodiversity $S(P(R),R)$ has stratification for different diseases and has a logarithmic growth with increasing the number of channels R as in Fig.8. We show that biodiversity can give very sensitive criterion for estimations of health status and variability of health in natural conditions and in medical treatment as in Figs.8 and 17.

We introduce Shannon entropy $S(J(R),R)$ for frequency of information J_m.We always observed, within experimental error, nearly the same dependence of $S(J(R),R)$ on R at all Figs.13,19,20 for any donors, regardless of time and health. This means the presence of homeostasis for information entropy $S(J(R),R)$ in oxidative activity of DNA for all neutrophils' populations in all living people.

We haven't met a Gaussian statistics in oxidative activity of DNA. We have a complex insufficiently multi-scales and multifractal networks in immunofluorescence based on distributions of flashes P_m, information J_m and entropy S_m. Standard statistical methods failed. For instance, the difference in histograms in Fig.14a is determined by the statistical instability of local distributions of fluorescence (see the exponential growth for moments of intensity fluctuations $M(i,k)$ in Fig.2) and cannot serve as an example of significant changes in populations of neutrophils or in health statuses for one given donor. Selection, isolation and differs only in central regions of histograms for the evidence of their difference has no legitimate basis.

Brokenness of histograms and corresponding fractal networks of immunofluorescence are more important than the characteristics of averages <I>, $<(I-<I>)^2>$ and so on. For example, stratifications of Hurst indices $H(S(P(R)),R)$ for frequencies of Shannon-Weaver index S_m in Fig.12 clearly define strong differences in the health of donors.

We observe the negative Hurst index H(P(R),R) for frequencies of flashes P_m and negative Hurst index H(S(R),R) for frequencies of entropy S_m in the case of low level of R in Figs.10,12,18 and 24. These situations correspond to abnormal Hausdorff dimension $D_H > 2$ and negative multifractal spectra [15]. Therefore, a complexity of

immunofluorescence networks and interlocking hierarchies with different scales is higher than descriptions of hierarchy networks for oxidative metabolisms in textbooks.

Immunofluorescence reflects simultaneously the genetic special, individual features and immune response to the pathogenic actions. Immunofluorescence data analysis is important for general estimation of health statuses and early diagnostics of diseases. Spectrum of medical applications is considerably wider, because of wide prevalence of oxidative abnormality as the reason of various illnesses and aging.

ACKNOWLEDGMENT

Specially thanks to M. Filatov for the kindly furnished experimental data.

REFERENCES

[1] J.P. Robinson, W. O Carter, P. K. Narayanan, "Oxidative product formation analysis by flow cytometry." In: *Methods in Cell Biology*, Vol 41, eds. Z. Darzynkiewicz, J.P. Robinson, H.A. Crissman (Academic press ,San Diego 1994), pp.437-447.

[2] M.V.Filatov, E. Y. Varfolomeeva, E.A. Ivanov, "Flow cytofluorometric detection of inflammatory processes by measuring respiratory burst reaction of peripheral blood neutrophils," *Biochemical and molecular medicine* vol.55, pp.116-121, 1995

[3] C.F. Bassoe, Li Nianyu, K Ragheb, G. Lawler, J. Sturgis, J.P. Robinson, "Investigations of Phagosomes, Mitochondria, and Asidis Granules In Human Neutrophils Using Fluorescence Probes," *Cytometry Part B (Clinical Cytometry),*vol. 51B, pp. 21-29, 2003

[4] H.M..Shapiro. *Practical Flow Cytometry* John Wiley &Sons, New York, 2003

[5] W. Weaver, C.E. Shannon, *The Mathematical Theory of Communication* University of Illinois, Urbana, 1949

[6] I.I. Eliazar1, I. M. Sokolov, "Diversity of Poissonian populations." *Phys.Rev.E*, vol.81, P.011122, 2010

[7] J. Feder, *Fractals* Plenum Press NewYork, 1988

[8] N.E.Galich**, "**Cytometric Distributions and Wavelet Spectra of Immunofluorescence Noise in Medical Diagnostics ," *eds* . O. Dossel and W.Schlegel (Eds.): WC 2009, IFMBE Proceedings 25/IV, Springer Berlin Heidelberg , pp. 1936–1939,2009

[9] I.D .Vladescu, M.J. McCaule, I. Rouzina , M.C. Williams, "Mapping the phase diagram of single DNA molecules forced-induced melting in the presence of ethidium," *Phys. Rev. Lett.*, Vol. 95, P. 158102, 2005

[10] N.E.Galich, M.V.Filatov, "Laser Fluorescence Fluctuation Excesses in Molecular Immunology Experiments," *Proc. SPIE*, Vol. 6597, P. 6597OL, 2007

[11] N.E.Galich, M.V. Filatov, "Delay, change and bifurcation of the immunofluorescence distribution attractors in health statuses diagnostics and in medical treatment.," *Proc. SPIE* Vol. 7377, 73770C Jun. 16, 2009

[12] N.E.Galich, " Bifurcations of averaged immunofluorescence distributions due to oxidative activity of DNA in medical diagnostics," (Accepted for publication), *Biophys.rev.lett.,* to be published ,2010

[13] Haiyuan Yu¤, Yu Xia¤, V. Trifonov and M. Gerstein, ".Design principles of molecular networks revealed by global comparisons and composite motifs," *Genome Biology*, vol.7**:**R55 m(doi:10.1186/gb-2006-7-7-r55),2006

[14] R. T. Glinton, P. Scerri, K. Sycara, " Towards the Understanding of Information Dynamics in Large Scale Networked Systems,"*Information fusion.2009.fusion'09.12-th International conference.6-9 July* ,Seattle, WA pp. 794 – 801, 2009

[15] Benoit B. Mandelbrot , "Multifractal Power Law Distributions: Negative and Critical Dimensions and Other ''Anomalies,''Explained by a Simple Example," *Journal of Statistical Physics*, Vol.110, Nos. 3–6, March,pp.739-774, 2003